A MRI myocardial perfusion analysis tool

Guillaume Née, Stéphanie Jehan-Besson, Luc Brun, Marinette Revenu, Martial Hamon, Michèle Hamon-Kérautret, Muriel Perrin

A MRI myocardial perfusion analysis tool

G. Née[1,4], S. Jehan-Besson[2], L. Brun[1], M. Revenu[1], M. Hamon[3], M. Hamon-Kérautret[3], M. Perrin[4]
[1] GREYC laboratory - CNRS UMR 6072 - Caen - France
[2] LIMOS laboratory - CNRS UMR 6158 - 63173 Aubière cedex, France.
[3] CHU - Caen - France
[4] General Electric Healthcare - Velizy - France

Abstract— **MRI myocardial perfusion analysis is an important element for the ischemic heart disorder assessment. The spatio-temporal analysis of the myocardial raising during the first crossing of a contrast bolus allows to identify the ischemic or hypo-perfused areas. Such an analysis requires an accurate tracking of the myocardium on the whole sequence and a robust segmentation to identify pathological and healthy regions inside the myocardium. In this paper, we present a semi-automatic tracking tool together with a segmentation algorithm based on statistical tests and a recent concentration theorem. Experimental results on both the tracking and segmentation of hypo-perfused areas confirm the availability of this setting.**

I. Introduction

The analysis of myocardial perfusion constitutes a key element in the evaluation of cardiac diseases. In this context, perfusion MRI (p-MRI) has emerged as a primordial clinical investigation tool because of its non invasive property. Spatio-temporal analysis of myocardial dynamics during the first transit of a contrast agent (Gadolinium) allows the identification of hypo-perfused or ischemic regions. The analysis of myocardial perfusion is up to now purely visual without any quantitative evaluation. In this paper, we present an automatic tracking of the cardiac structures and a merging algorithm for the segmentation of hypo-perfused regions. This work[1] constitutes the first step of a larger project whose goal is to quantify the spatio-temporal repartition of the image intensity in the myocardium.

The main difficulty for the segmentation of cardiac structures in p-MRI sequences lies in the fact that the different regions (myocardium, left ventricle) encounter strong variations of intensity due to the transit of the contrast agent. Besides, even if the images are taken at instants corresponding to the same phase of the cardiac cycle, a registration is needed due to the patient breathing [13]. The registration is classically performed on the whole image [3].

Instead of a registration of the whole frame, we rather track the contours of the cardiac structures along the sequence as in [10]. We present in this paper our tracking algorithm and we complete this study by the proposition of a myocardial hypo-perfused region segmentation algorithm. The tracking algorithm is robust and efficient and is realized in two main steps: (i) a local motion estimation based on an improved block matching method inspired from video compression standards [14] and (ii) from this local motion estimation, we deduce the affine transformations of both epicardium and endocardium contours. In order to identify accurately the myocardial hypo-perfused regions, we propose the use of a region growing algorithm based on a graph representation. This method requires the design of a merging predicate in order to decide if the the two selected regions must be merged or not and the design of a merging order to iteratively select couples of regions that must be tested by our predicate. This predicate is designed using a contrario approaches [4] and the recent statistical inequality of McDiarmid [9].

The paper is organized as follows. The tracking algorithm is detailed in section II. Section III presents our region growing segmentation algorithm. Finally, we present our experimental results for a complete analysis of myocardial perfusion in section IV.

II. Tracking

We propose to track the contours of the myocardium throughout the whole sequence. The initial segmentation can be performed manually by an expert or automatically in an image of high contrast using for example region-based active contours [2], [8]. In this paper, segmentation is performed manually in a first frame and the contours of the region are then approximated using Bézier curves and deformed from one frame to another using a global affine parametric model. The estimation is performed in two main steps : first, we estimate motion vectors using an improved block matching algorithm explained in section II-A and then, we deduce from this estimation a global parametric transformation (section II-B) which is applied to deform the curves from one frame to another. This algorithm allows a robust and efficient segmentation at a low computational cost.

A. Local motion estimation

Local motion estimation between two successive images is performed using an improved block-matching algorithm which includes blocks of variable sizes as in [14] and a robust similarity criterion invariant to affine variations of intensities. Indeed, the similarity criterion between two blocks must be chosen so as to compensate the variation of intensities inside the cardiac regions (myocardium and left ventricle) due to the transit of the contrast agent. In order to find the displacement $d(p)$ of the pixel p, we minimize the *ZNSSD* (Zero-mean Normalized Sum of squared Differences)

[1]This work is funded by a grant cofinanced by General Electric Healthcare and the Region Basse Normandie. Images from this paper come from the radiology service of the CHU of Caen (Normandy, France).

criterion defined as follows:

$$ZNSSD(d) = \frac{1}{|B|} \frac{\sum_{p\in B} \left[I_t(p) - \overline{I_t(p)} - \left(I_{t+1}(p+d) - \overline{I_{t+1}(p+d)} \right) \right]^2}{\sqrt{\sum_{p\in B} \left(I_t(p) - \overline{I_t(p)} \right)^2 \sum_{p\in B} \left(I_{t+1}(p+d) - \overline{I_{t+1}(p+d)} \right)^2}} \quad (1)$$

where B designates a block of size $|B|$ that contains the pixel $p = (x,y)^T$ and the term $d(p) = (d_x(p), d_y(p))^T$ represents the displacement of the pixel p. This criterion presents the advantage to be invariant to affine variations of intensities between two blocks.

Blocks are usually defined by dividing the image frame into non-overlapping square parts. In this work, in order to improve the accuracy of motion estimation, we authorize variable sizes of blocks as in advanced encoding schemes (e.g. H264, MPEG-4 AVC). If the ZNSSD of a block is greater than a threshold α and if the sum of the gradients along the x-axis $S_x = \frac{1}{|B|} \sum_{p\in B} |\nabla_x(p)|$ is greater than a threshold β, we split the block in two vertical sub blocks of equal size. In the same way, the block is splited horizontally if its ZNSSD is above α and the sum of gradients along the y-axis S_y is greater than the threshold β.

B. Global motion computation

We assume that cardiac structures undergo a parametric transformation $\mathbf{T}$ from one frame to another. We propose to estimate this transformation by minimizing the following criterion:

$$E(\mathbf{T}) = \sum_{p\in\Omega_I} \varphi(||d(\mathbf{p}) - \mathbf{T}(\mathbf{p})||)$$

where d is the motion vector estimated in the previous section and Ω_I is the image domain.

In this study, we use a six parameters affine model for the transformation $\mathbf{T}$. The function φ is chosen as $\varphi(r) = r^2$, in order to guarantee the uniqueness of the solution.

The estimated parametric transformation $\mathbf{T}$ is applied to each point of the curves from one frame to another, performing in this way an elastic deformation.

III. Hypo-perfused region segmentation

In order to quantify the perfusion, medical experts usually separate the myocardium in segments using the 3 SA-levels, 16-segments LV model recommended by the American Heart Association (AHA)[1], this method is used for example by [5].

In this part, we propose a segmentation tool that allows to accurately delineates the hypo-perfused region inside the myocardium and then its precise repartition in the different segments and the corresponding myocardial hypo-perfused ratio. We propose in this work to segment hypo-perfused regions using a region growing algorithm based on significance tests and on the recent statistical inequality of McDiarmid [9]. Our algorithm can be seen as an extension of the work proposed in [12] with an improved merging order. As in [6], we also propose to define it using a contrario principles.

A. Problem statement

Due to the random part in image acquisition systems, an image I is classically considered as an observation of a perfect statistical image I^*. Using such an image model, an ideal region is defined as a vector $\mathbf{X} = (X_1, \ldots, X_n)$ of n random variables representing the pixel intensities. A "real" region is then considered as an observation of this random vector which takes its values in $\prod_{k=1}^{n} A_k$. In natural images, the set of admissible values A_k usually corresponds to $[0;M]$ where $M = 255$. However, in medical images (e.g.: MRI, Echography), the set A_k may be larger.

Segmentation using a region growing algorithm is realized through the definition these two main items:

- A merging predicate $P(X_i, X_j)$ which decides if two adjacent regions $\mathbf{X}_i$ and $\mathbf{X}_j$ have to be merged or not. Such a merging predicate is generally based on a dissimilarity measure and a similarity hypothesis.
- A merging order which defines an order to be followed to check the merging predicate.

The design of these two points is crucial for segmentation purposes. Let us now introduce our general framework to compute such merging predicates based on a contrario approaches and recent statistical inequalities. The merging order (given in section III-E) will be deduced from the merging predicate.

B. Problem statement using a contrario approaches

Given two statistical regions $\mathbf{X}_1$ and $\mathbf{X}_2$ and a dissimilarity criterion $d(.,.)$, let us consider two observations R_1 and R_2 of respectively $\mathbf{X}_1$ and $\mathbf{X}_2$ and the event E: *the observed value* $d(R_1,R_2)$ *of the statistic* $d(\mathbf{X}_1,\mathbf{X}_2)$ *is greater than a threshold* T. The a contrario approach is based on the estimation of the probability of this event under the similarity hypothesis $\mathbf{H_0}$. Let us consider an upper bound δ of this probability:

$$\mathbf{P}\{d(\mathbf{X}_1,\mathbf{X}_2) \geq T | \mathbf{H_0}\} \leq \delta \quad (2)$$

We can remark that the probability δ and the threshold T are dependent. Indeed if the threshold T is set to a high value, this corresponds to a non probable event under $\mathbf{H_0}$ and δ should then be small. On the contrary if the threshold T is set to a small value, this corresponds to a probable event under $\mathbf{H_0}$ and so δ must be large. Usually, one may assume that the threshold T is a decreasing function of δ which may be denoted as $T(\delta)$.

Using the a contrario approach, if we take δ as a low probability value, the event E is considered as not probable under the similarity hypothesis $\mathbf{H_0}$ and this hypothesis is then rejected. Our decision rule for region merging is then defined as:

$$\text{if} \quad d(R_1,R_2) \geq T(\delta) \quad \text{then} \quad \mathbf{H_0} \text{ is rejected} \quad (3)$$

and then R_1 and R_2 are observations of two distinct statistical regions $\mathbf{X}_1$ and $\mathbf{X}_2$ and must not be merged.

C. Thresholds computation using concentration inequalities

The main difficulty of the above approach lies in the computation of the threshold $T(\delta)$. In this work, we propose to use the extension of the McDiarmid theorem [9] which allows to bound the probability of a large class of events. Let us remind this theorem:

Theorem 3.1: Let $\mathbf{Y} = (Y_1, \ldots, Y_n)$ be a family of random variables with Y_k taking values in a set A_k, and let f be a bounded real-valued function defined on $\Omega = \prod_{k=1}^{n} A_k$. If μ denotes the expectation of $f(\mathbf{Y})$ we have for any $\alpha \geq \mu$:

$$\mathbf{P}\{f(\mathbf{Y}) \geq \alpha\} \leq \exp\left(\frac{-2(\alpha-\mu)^2}{r^2}\right) + \mathbf{P}\{\mathbf{Y} \in C\} \quad (4)$$

Where C is a subset of Ω and r^2 is the maximal sum of squared range defined on $\overline{C} = \Omega - C$.

The set C in the above theorem corresponds to a set of outliers for $\mathbf{Y}$. Within our framework, we define $f(Y)$ as our dissimilarity measure $d(\mathbf{X}_1, \mathbf{X}_2)$ and Y as an appropriate combination of the two vectors $\mathbf{X}_1$ and $\mathbf{X}_2$.

Let us denote by $\Delta(\alpha)$, the probabilistic bound given by the McDiarmid's theorem:

$$\mathbf{P}\{f(\mathbf{Y}) \geq \alpha\} \leq \Delta(\alpha) \quad (5)$$

The threshold $T(\delta)$ introduced in (2) can then be estimated by setting $\delta = \Delta(\alpha)$ and so $\alpha = \Delta^{-1}(\delta)$.

D. Piecewise constant predicate

We measure the similarity between the two regions by the following dissimilarity measure:

$$f(\mathbf{X}) = d(\mathbf{X}_1, \mathbf{X}_2) = |U_1 - U_2| \quad (6)$$

where $\{U_j\}_{j=1;2}$ denote the random variables corresponding to the means of the statistical regions $\{\mathbf{X}_j\}_{j=1;2}$ of associated sizes $|\mathbf{X}_j|$.

Our goal is to compute a decision rule that indicates if two observations R_1 and R_2 of $\mathbf{X}_1$ and $\mathbf{X}_2$ are similar or not. According to our approach, we have to upper bound the probability that the function $f(\mathbf{X}) = d(\mathbf{X}_1, \mathbf{X}_2)$ is greater than a given threshold α using the McDiarmid's theorem (theorem 3.1). Such an upper bound is provided by the following proposition:

Proposition 3.1: Using the previously defined notations, we have for any couple $(\mathbf{X}_1, \mathbf{X}_2)$ of statistical similar regions and any threshold $\alpha > 0$:

$$\mathbf{P}\{d(\mathbf{X}_1, \mathbf{X}_2) \geq \alpha\} \leq \exp\left(-\frac{2|\mathbf{X}_1||\mathbf{X}_2|}{g^2(|\mathbf{X}_1| + |\mathbf{X}_2|)}(\alpha-\mu)^2\right) + K \quad (7)$$

with $K = \mathbf{P}\{\mathbf{X} \in C\}$ where $C \subset \Omega$ is the set of outliers. If $C_\Omega^c = [N; N']$ defines the complementary of C in Ω, then $g = N' - N$.

See [11] for a similar proof of this proposition.

The parameter g must be chosen such that the probability K can be ignored. In this work, we use $g = \max_{\mathbf{x} \in |I|} I(\mathbf{x}) - \min_{\mathbf{x} \in |I|} I(\mathbf{x})$ which ensures a negligible value of K compared to δ. The parameter μ may be estimated using an assumption on the noise model. In MRI sequences the noise model is assumed to follow a Rician distribution [7]. For large signal intensities the noise distribution can be considered as Gaussian ($X_i \sim \mathcal{N}(m_i, \sigma)$ for $1 \leq i \leq N$). In this case, the expectation of the function f can be computed which leads to:

$$\mu = \frac{2\sigma\left(\sqrt{|\mathbf{X}_1|} + \sqrt{|\mathbf{X}_2|}\right)}{\sqrt{2\pi|\mathbf{X}_1||\mathbf{X}_2|}} \quad (8)$$

This computation is simply made using well-known properties for the combination of Gaussian models.

Given two observations R_i, R_j of two statistical regions X_i and X_j, the merging is guided by the following predicate:

$$P(R_i, R_j) = \begin{cases} \text{true} & \text{if } |\overline{R_i} - \overline{R_j}| \leq \alpha_{ij}(\delta) \\ \text{false} & \text{otherwise} \end{cases} \quad (9)$$

with $\alpha_{ij}(\delta) = g\sqrt{\frac{|R_i| + |R_j|}{2|R_i||R_j|} \ln\left(\frac{1}{\delta - K}\right)} + \mu$.

Compared to the approaches [12], [6], we do not make the assumption that in the same statistical regions $E[U_1 - U_2] = 0$. In fact, this is not the case for noisy images. Using equation (8), we can remark that such an assumption is only valid under the law of large number and is not verified for small regions. This last point is illustrated in our experimental results.

E. Merging algorithm

Following our general setting for the computation of the merging predicate, let us now introduce the whole segmentation algorithm that includes an original merging order.

Given an image I, the regions adjacency graph (RAG) $\mathscr{G}$ is composed of a set of vertices $\mathscr{V}$ representing the observed regions (initially reduced to a single pixel) and a set of edges $\mathscr{E}$ encoding the adjacency of regions in 4-connexity. A weighted edge is then a triplet composed of a couple of nodes (v_i, v_j) with their corresponding weight w_{ij}. In our work, this weight is defined as the ratio of the value of the criterion (left side of (9)) and the computed threshold (right side of (9)) as follows:

$$w_{ij} = \frac{|\overline{R_i} - \overline{R_j}|}{\alpha_{ij}(\delta)} \quad (10)$$

Using the above formula, the predicate P between 2 regions R_i and R_j is true if and only if the edge e_{ij} between the associated vertices v_i and v_j is lower than 1. Our merging order on the edges e_{ij} corresponds to a decreasing order on the probability of $d(R_i, R_j) > \alpha_{ij}$ (Eq. (7)). One may show that such a merging order is equivalent to an increasing order on the edges weights.

The merging order is updated efficiently during the merging process using a heap structure combined with an index which associates to each edge its indice in the heap.

IV. Experimental Results

Our database is composed of five p-MRI sequences. Each p-MRI sequence has been acquired sequentially on five levels along the little axis at instants corresponding to the same

phase of the cardiac cycle. We have thus 25 sequences of 2D images. We present here a result obtained on a p-MRI sequence corresponding to an important breathing movement.

A. Cardiac regions tracking

The myocardium has been manually segmented on frame #15 of the heart's basal level and has been tracked all along the perfusion sequence (backward and forward). Concerning the local motion estimation step, the initial block size has been set to 32×32 and can be divided until a size of 16×16. The values of α and β have been respectively set to 1 and 5. To present the results of our tracking algorithm, we have extracted four frames from the basal level perfusion sequence after registration (Fig. 1).

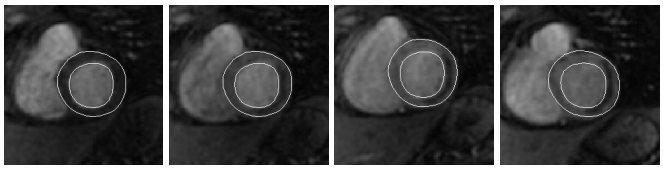

Fig. 1. Tracking of cardiac structures using our tracking algorithm - from left to right: tracking results on frames #16, #24, #30 and #40.

B. Segmentation of hypo-perfused regions

In Fig. 2, we display the results of our segmentation algorithm on 3 frames of the same p-MRI sequence. These results have been obtained by setting the unique parameter $\delta = 0.4$. From this segmentation, the proportion of hypo-perfused areas inside the myocardium has been automatically estimated to $10,97\%$, $10,26\%$ and $6,7\%$ for respectively frames #30, #39 and #44. The myocardium is also divided following the model recommended by the American Heart Association. Combining this last model with our segmentation results leads to the identification of the corresponding supplying artery.

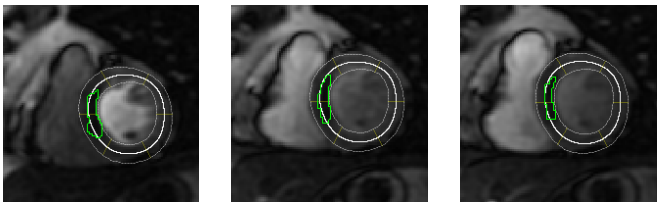

Fig. 2. Temporal segmentation of hypo-perfused region inside the myocardium (frame #30, #39 and #44).

Fig. 3 shows the segmentation of hypo-perfused regions using the algorithm from [6] on the left and our one on the right. The left segmentation result has been obtained by setting $\delta = 0.1$, it is composed of 5 regions. The right one has been obtained by setting $\delta = 10^{-4}$ and gives 4 regions, the standard deviance of the noise has been estimated to $\sigma = 35.36$ and the parameter $g = 7040$. We can see that the hypo-perfused region (low contrast on the right side of the myocardium) is accurately segmented by our method while the other method does not perfectly enclosed the region.

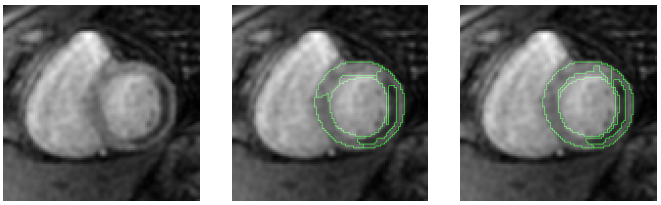

Fig. 3. Segmentation of hypo-perfused regions inside the myocardium in MRI perfusion imaging using respectively the algorithm from [6] (second column) and our one (third column).

V. Conclusion

In this paper, we have proposed an efficient and robust tracking algorithm of the cardiac structures along p-MRI sequences and a region growing segmentation algorithm designed to segment small and accurate regions of interest. These two algorithms constitute a first step towards an accurate characterization of quantification parameters. Our on-going research is directed towards the computation of quantification parameters from such a segmentation.

References

[1] M. D. Cerqueira, N. J. Weissman, V. Dilsizian, A. K. Jacobs, S. Kaul, Laskey, and al., "Standardized myocardial segmentation and nomenclature for tomographic imaging of the heart." *Circulation*, vol. 105, no. 4, pp. 539–542, January 2002.

[2] T. Chan and L. Vese, "Active contours without edges," *IEEE Transactions on Image Processing*, vol. 10, no. 2, pp. 266–277, 2001.

[3] T. Delzescaux, F. Frouin, A. de Cesare, P.-F. S., A. Todd-Pokropek, A. Herment, and M. Janier, "Using an adaptive semiautomated self-evaluated registration technique to analyze MRI data for myocardial perfusion assessment," in *J. Magn. Reson. Imaging*, vol. 18(6), 2003, pp. 681–690.

[4] A. Desolneux, L. Moisan, and J.-M. Morel, "A grouping principle and four applications," *PAMI*, vol. 25, no. 4, pp. 508–513, 2003.

[5] A. Discher, N. Rougon, and F. Prêteux, "An unsupervised approach for measuring myocardial perfusion in mr image sequences," in *SPIE Conference on Mathematical Methods in Pattern and Image Analysis, San Diego, CA*, vol. 5916, August 2005, pp. 126–137.

[6] M. E. Hassani, S. Jehan-Besson, L. Brun, and al., "Time-consistent video segmentation algorithm designed for real-time implementation," *VLSI Design*, 2008.

[7] R. Henkelman, "Measurement of signal intensities in the presence of noise in MR images," *Med. Phys.*, vol. 12, pp. 232–233, 1985.

[8] S. Jehan-Besson, A. Herbulot, M. Barlaud, and G. Aubert, *Mathematicals Models of Computer Vision : The Handbook*. Springer, 2005, ch. Shape gradient for image and video segmentation, pp. 309–323.

[9] C. McDiarmid, "Concentration," in *Probabilistic Methods for Algorithmic Discrete Mathematics, Springer*, M. Habib, C. McDiarmid, J. Ramirez-Alfonsin, and B. Reed, Eds., 1998.

[10] F. P. N. Rougon, A. Discher, "Region-based statistical segmentation using informational active contours," in *SPIE Conference on Mathematics of Data/Image Pattern Recognition, Compression, and Encryption with Applications IX, San Diego, CA*, vol. 6315, August 2006, pp. 63 150I–1:12.

[11] G. Née, S. Jehan-Besson, L. Brun, and M. Revenu, "Significance tests and statistical inequalities for region matching," in *Joint IAPR International Workshops S+SSPR 2008*, ser. Lecture Notes in Computer Science, N. da Vitaro Lobo et al., Ed., vol. 5342. Springer, December 2008, pp. 350–360.

[12] R. Nock and F. Nielsen, "Statistical region merging," *IEEE PAMI*, vol. 26, no. 11, pp. 1452–1458, November 2004.

[13] M. B. Stegmann, H. Ólafsdóttir, and H. B. W. Larsson, "Unsupervised motion-compensation of multi-slice cardiac perfusion MRI," *Medical Image Analysis*, vol. 9(4), pp. 394–410, 2005.

[14] T. Wiegand, G. Sullivan, G. Bjntegaard, and A. Luthra, "Overview of the H.264/AVC video coding standard," *IEEE Transactions on Circuits and Systems for Video Technology*, vol. 13, no. 7, pp. 560–576, 2003.